3-1-2006

Tailorable, 3D microfabrication for photonic applications: Two-polymer microtransfer molding

Jae-Hwang Lee
Iowa State University

Chang-Hwan Kim
Iowa State University

Kristen P. Constant
Iowa State University, constant@iastate.edu

Kai-Ming Ho
Iowa State University, kmh@ameslab.gov

Tailorable, 3D microfabrication for photonic applications: Two-polymer microtransfer molding

Jae-Hwang Lee[*a, b], Chang-Hwan Kim[a,b], Kristen Constant[a,c], and Kai-Ming Ho[a,b]
[a]Ames Laboratory-USDOE, Ames, IA, USA 50011
[b]Department of Physics and Astronomy, Iowa State University, Ames, IA, USA 50011
[c]Department of Materials Science and Engineering, Iowa State University, Ames, IA, USA 50011

ABSTRACT

For photonic devices, extending beyond the planar regime to the third dimension can allow a higher degree of integration and novel functionalities for applications such as photonic crystals and integrated optical circuits. Although conventional photolithography can achieve both high quality and structural control, it is still costly and slow for three-dimensional (3D) fabrication. Moreover, as diverse functional polymers emerge, there is potential to develop new techniques for quick and economical fabrication of 3D structures. We present a 3D microfabrication technique based on the soft lithographic technique, called two-polymer microtransfer molding (2P-μTM) to accomplish low cost, high structural fidelity and tailorable 3D microfabrication for polymers. Using 2P-μTM, highly layered polymeric microstructures are achievable by stacking planar structures layer by layer. For increased processing control, the surface chemistry of the polymers is characterized as a function of changing ultraviolet dosage to optimize yield in layer transfer. We discuss the application of the 2P-μTM to build polymer templates for woodpile photonic crystals, and demonstrate methods for converting the polymer templates to dielectric and metallic photonic crystal structures. Finally, we will show that 2P-μTM is promising for fabricating 3D polymeric optical waveguides.

Keywords: Microfabrication, photonic crystal, three-dimensional, soft lithography, microtransfer molding, polymer microstructure

1. INTRODUCTION

Attempts to miniaturize photonic devices require novel classes of materials such as three-dimensional photonic crystals [1] to realize photonic circuits at a scale comparable to the wavelength of guided light. There are numerous fabrication methods for photonic crystals in the optical regime [2-5]. To reduce the costs and complexities of fabrication, approaches using non-photolithographic techniques, such as microtransfer molding (μTM) [6, could be an alternative to pre-existing techniques. In μTM, a liquid prepolymer is filled in a micro-relief structure formed on the surface of an elastomeric mold and cured after placing it in contact with a substrate. The cured prepolymer remains on the substrate surface when the elastomeric mold is peeled off. Since highly layered structures are necessary for photonic crystals, the yield in a layer transfer step is critical. In this report we present an advanced μTM technique to accomplish high fabrication yield and high structural fidelity, called two-polymer microtransfer molding (2P-μTM) [7]. Using 2P-μTM, we fabricated polymeric templates for woodpile photonic crystals, and converted the templates to metallic and ceramic photonic crystals. In addition to photonic crystals, submicron-optical waveguides has become a promising element in integrated photonic devices for communication and bio-sensing [8-10]. We also demonstrate the capability of 2P-μTM to realize tailorable and flexible optical waveguide arrays in the visible region.

2. EXPERIMENTAL AND RESULTS

A photoresist (AZ 5214, Clariant) relief structure was patterned on a silicon wafer using standard photolithography. The inverse replica of the relief structure was made by casting poly(dimethylsiloxane) (PDMS) elastomer (Sylgard 184, Dow Corning) on the relief structure. The mixing ratio of resin and hardener in the casting process was 10:1 by weight, and air bubbles captured in the mixture were removed in a vacuum chamber. After pouring the mixture on the relief structure and subsequently curing at 60 °C for 4 hours, the cured PDMS mold was simply peeled off. The patterned surface of the PDMS mold, the inverse replica of its original structure, was filled with a photo-curable prepolymer by a wet-and-drag (WAD) process as depicted in Figure. 1. In the WAD process, a drop of a liquid prepolymer is applied at

Photonic Crystal Materials and Devices IV, edited by Ali Adibi, Shawn-Yu Lin, Axel Scherer,
Proc. of SPIE Vol. 6128, 612805, (2006) · 0277-786X/06/$15 · doi: 10.1117/12.645303

the outside of a patterned area, and a sharp metallic blade was lowered to make contact with the prepolymer drop . Since the prepolymer adheres to the blade and spreads along the blade, we were able to move the prepolymer drop across the patterned surface of the PDMS mold. The distance between the blade and a surface of the PDMS mold was approximately 0.2 mm. As soon as the front boundary of the drop reaches the end of the patterned area, the blade moves backward to induce dewetting of the prepolymer. The WAD completes when the blade returns to its starting position. The droplet of the prepolymer can be removed easily because the droplet solidifies in the following curing step.

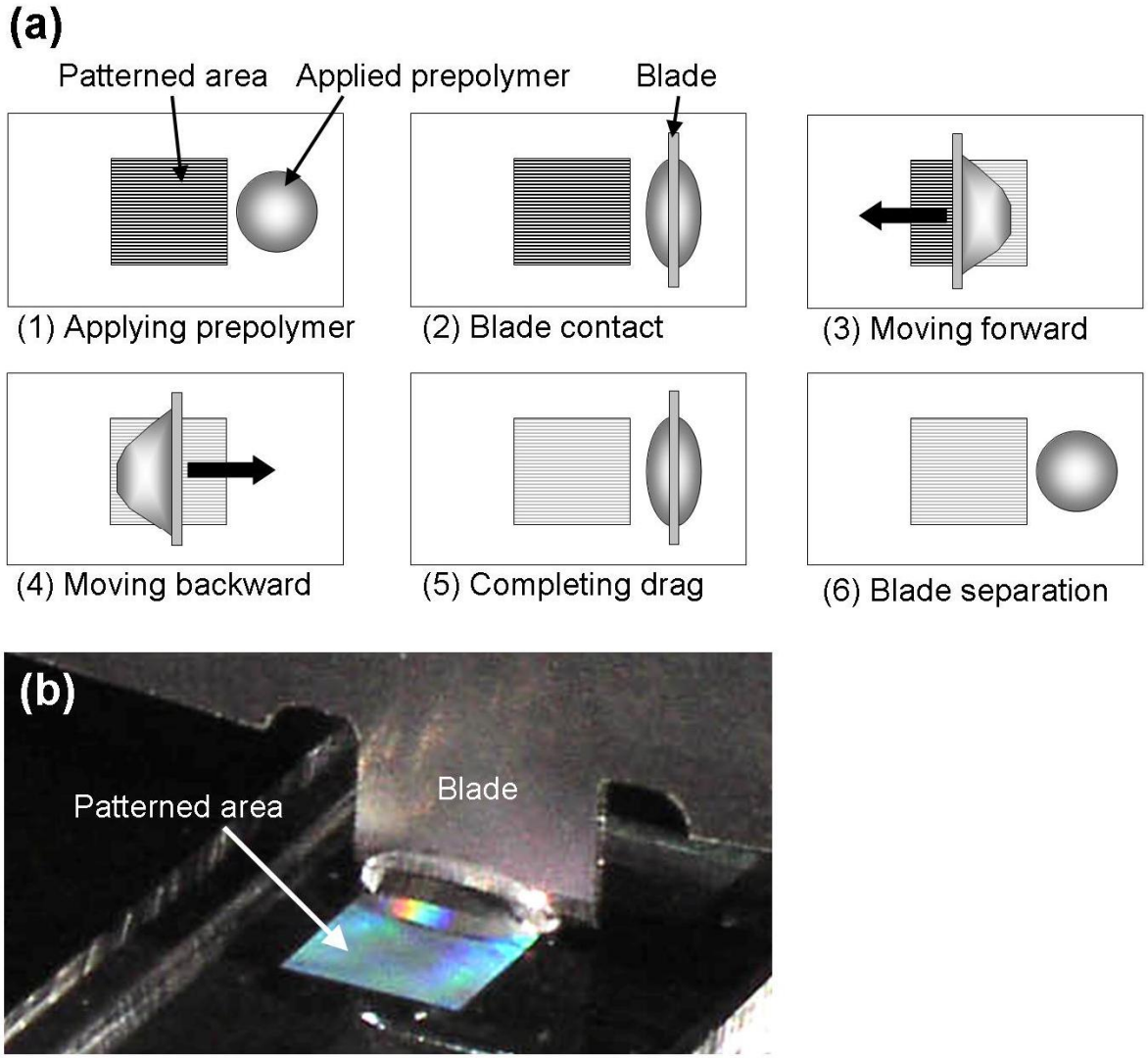

Fig. 1 (a) schematic of wet-and-drag and (b) a photograph of experimental apparatus in WAD.

We performed the WAD with different photo-curable prepolymers under the same conditions to find an appropriate prepolymer that shows optimal filling behavior. PDMS molds with different prepolymers were exposed to ultraviolet (UV) light and examined using a scanning electron microscope (SEM) immediately after completing the WAD process. Some of the results are shown in Figure 2. Polyurethane prepolymers (NOA 71 and NOA 73, Norland Products; J-91, Summers Optical) and poly metacrylate prepolymer (SK-9, Summers Optical) showed different results under the same processing conditions. In the SEM images, bright areas represent rough surfaces, i.e., under- or over- filled areas. Because the bright areas in the SEM image of the PDMS mold in Fig 2(c) are actually defects of the mold, transferred from its original pattern, we can infer that J-91 exhibits superior filling behavior among the prepolymers.

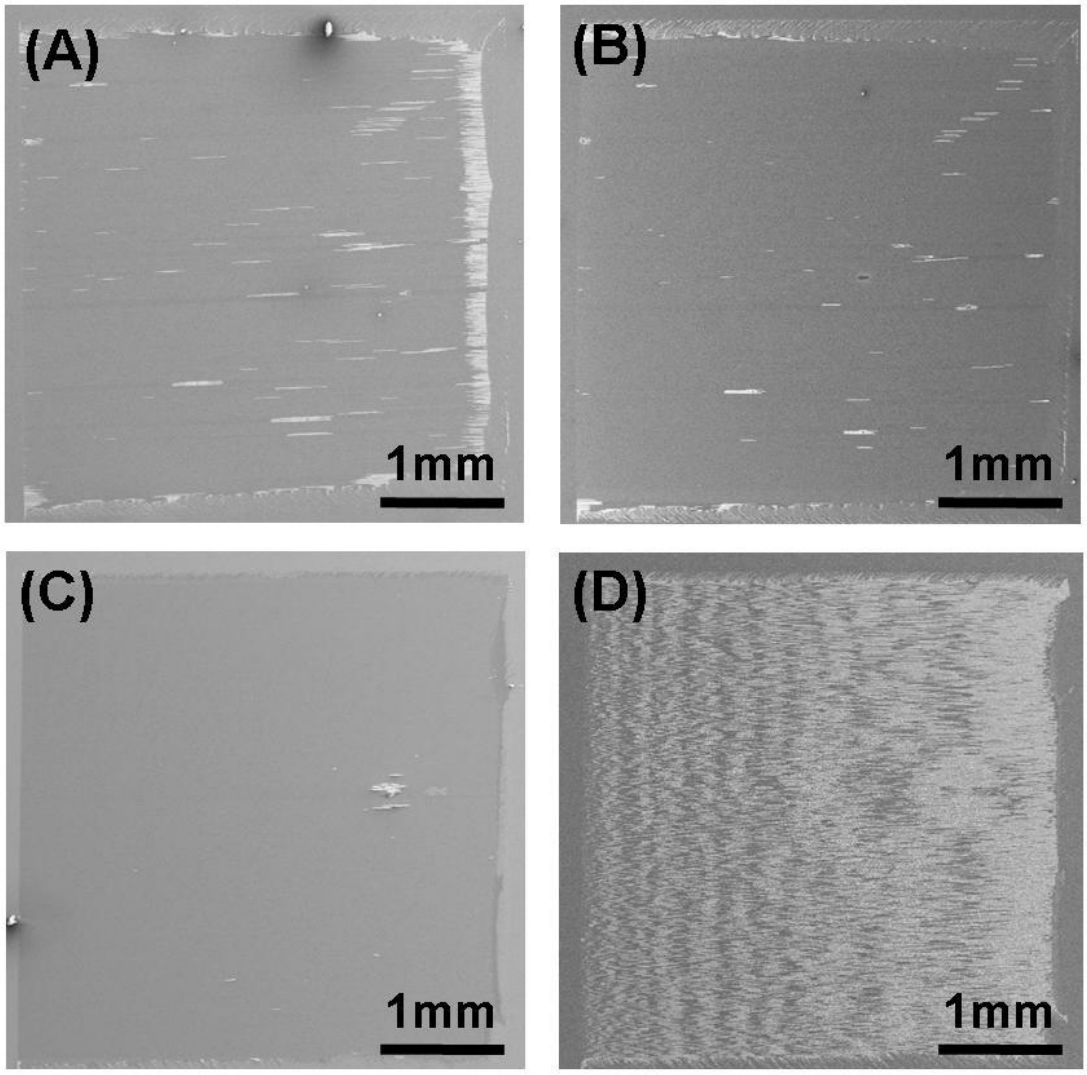

Fig. 2 SEM images of filled PDMS molds with (a) NOA 71, (b) NOA 73, (c) J-91 and (d) SK-9.

We find that a dragging speed of WAD of J-91 around 30μm/s allows complete filling of patterns on a PDMS mold while minimizing the swelling of the PDMS mold due to long time contact with J-91. Swelling of the PDMS mold hinders the release of polymer structures from the PDMS molds. We expose the PDMS mold to UV to solidify the filled prepolymer. The UV exposure reduces the possibility of capillary wicking upon contact with the substrates or layered structures. This leads to improvement of the fidelity of resultant structures. Another agent is required to provide adhesion of the solidified J-91. Without the additional bonding agent, we could not transfer the filled structure to other substrates. We used SK-9 as a bonding agent because of its low viscosity (80 cps) and high bonding strength to glass and polymers. The WAD of SK-9 was performed on a J-91 filled PDMS mold after UV exposure of J-91. Through WAD, SK-9 is coated only on the top surface of filled J-91. Noticeable changes were not detected in the SEM images taken before and after WAD of SK-9 in Figure 3. Because the coating thickness of SK-9 is much thinner than the filled structure, poor contact with a target surface would happen if the filling was not precise. We observed that J-91 filled each channel spontaneously with exact height and a flat meniscus. This filling behavior eliminates expensive and time consuming leveling steps such as chemical mechanical polishing and reactive ion etching.

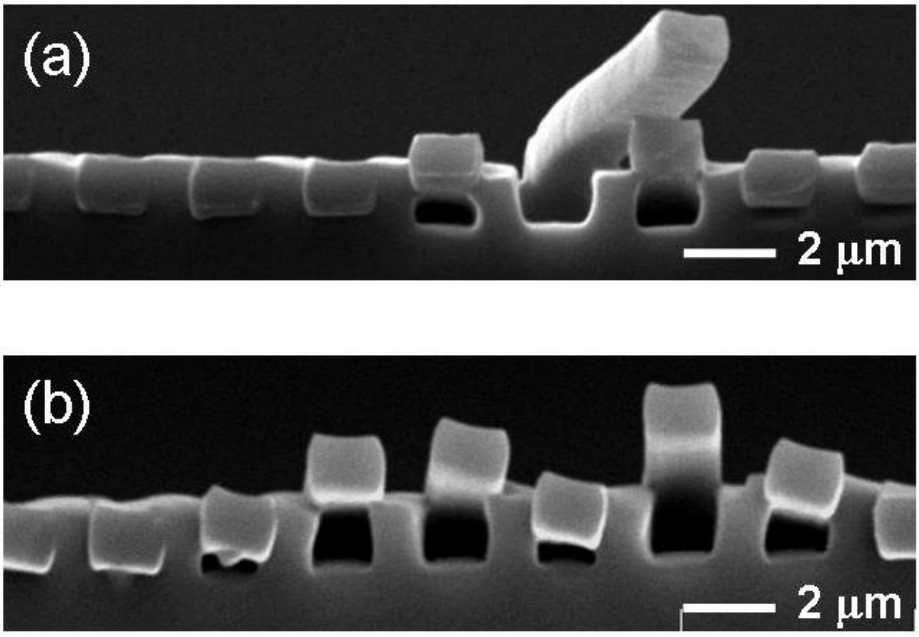

Fig. 3 Cross sectional SEM images of J-91 filled PDMS molds (a) before and (b) after WAD of SK-9.

The amount of coated SK-9 could be affected by the UV dosage for solidifying J-91. To estimate the correlation between the amount of coated SK-9 and the UV dosage, we doped SK-9 with a red dye (LDS 698, Excition). Photoluminescence (PL) from the doped SK-9 was measured after WAD of SK-9 as a function of UV exposure time for J-91. The intensity of a UV lamp used for curing of J-91 was 1.5 mW cm^{-2} at 366 nm, and line width of UV was 4.8 nm (full-width at half-maximum). The PL spectra from different UV doses fell into two groups as shown in black and gray lines in Figure 4(a). Since higher intensity of PL means larger amount of SK-9, we integrated each PL spectrum ranging from 550 nm to 800 nm. The correlation between the integrated value of each spectrum and corresponding exposure time is shown in Fig. 4(b). For the exposure times in the range from 5 to 30 minutes, a very low transfer-error rate below 10^{-4} was observed, where the transfer-error rate is defined by the ratio of the number of failed elements to the total number of elements to be transferred. In the range of exposure times, the shortest time, 5 minutes was selected to reduce the total process time.

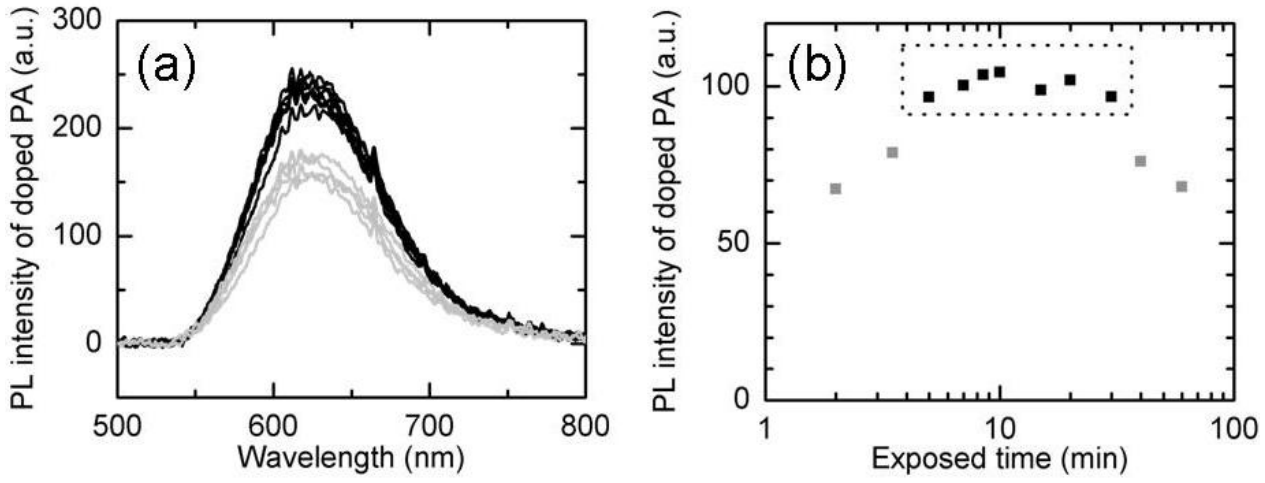

Fig. 4. (a) PL spectra of doped SK-9 after WAD; (b) Correlation between PL and UV exposed time. Black and gray dots correspond to the spectrum curves depicted as same colors in (a).

We repeated a single layer transfer on a pre-stacked structure with the optimal exposure time to demonstrate the capability of 2P-μTM. At each layer transfer, orientation of a layer was alternated to be perpendicular to the prior layer. The fabricated 12-layered microstructure in Figure 5 shows high structural fidelity as well as high layer-transfer yield. The lateral size of the 12-layered microstructure was 4 mm by 4 mm. The fabrication of the sample with many layers on a large area demonstrated the extremely high yield in our layer transfer process.

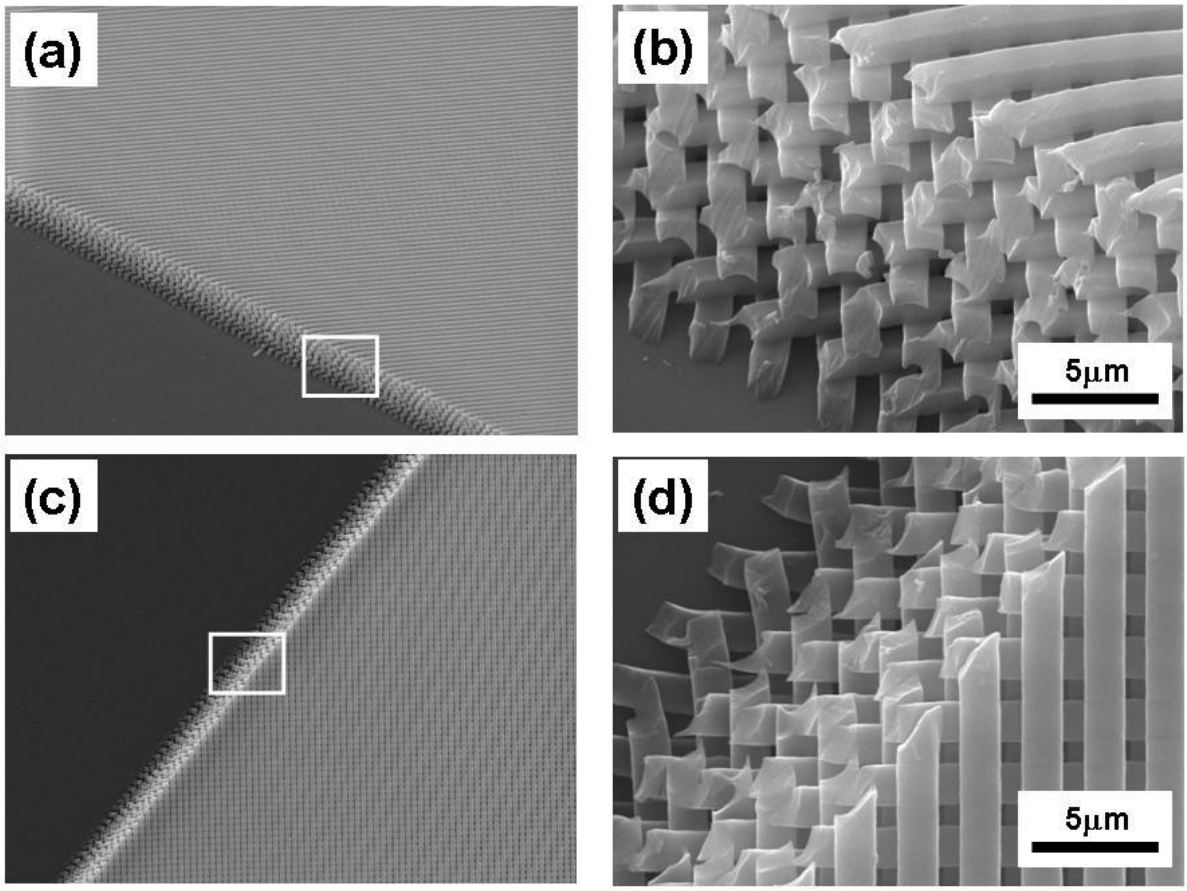

Fig. 5 SEM images of the 12-layered microstructure. Tilted and top view of the structure are shown in (a) and (c), respectively. The images, (b) and (d), are a close view of the structures in a white box in the images in the left panel.

We applied 2P-μTM to the fabrication of woodpile photonic crystals. In the fabrication of the photonic crystals, we used diffracted moiré fringes for alignment of additional layers to layers already fabricated [11]. The diffracted moiré fringe method enables alignment of transparent periodic micro-structures even when they have a low refractive index contrasts. By using metal deposition or ceramic infiltration, we successfully converted polymer structures to metallic or ceramic photonic crystals. For metallic photonic crystals, we used free-standing polymeric templates, which is fabricated by adding a sacrificial layer between the substrate and the polymer template. We deposited gold on the free-standing polymer templates thicker than the skin depth of gold at target wavelengths. For ceramic photonic crystals, ceramic slurries composed of titania nanoparticles were used as infiltration material. After infiltration, the polymer template was removed by heating. The converted metallic and ceramic woodpile photonic crystals are shown in Figure 6 as an example. From the SEM images we can see that the polymer structures can be converted to metallic and dielectric structures without loss of structural fidelity.

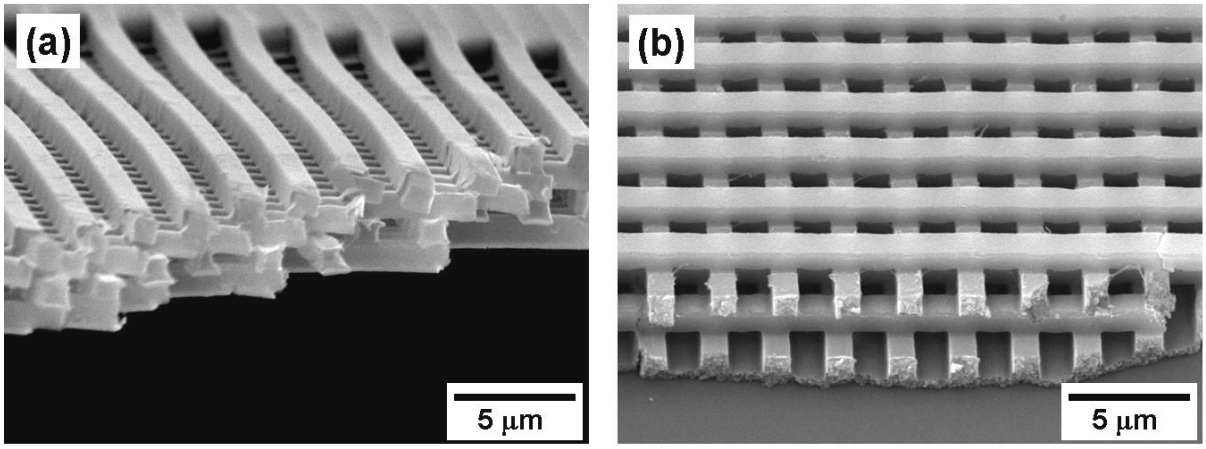

Fig. 6 Examples of (a) metallic and (b) ceramic photonic crystals, converted from their polymer template.

The cured J-91 is a good optical material to guide light due to its transparency, high refractive index (n=1.55) in visible wavelengths, and chemical stability. Because of these advantages, we can use each single rod as an optical waveguide. To demonstrate waveguiding capability, we fabricated an array of waveguides consisting of 1,600 individual polymer rods as shown in Figure 7(a). An oxidized silicon wafer was used as a substrate. Then, light sources were coupled into the waveguides at the end of the rods by depositing quantum-dot-containing resin with a stainless steel stylus. The quantum dot resin contains PbSe/ZnS core-shell nanoparticles, which have a peak emission at 625 nm. The quantum dots were excited by a focused UV beam (364 nm) from an argon ion laser. The experimental setup is shown in Fig. 7(b). By excitation of the quantum dots from top of the array, some of emitted light was coupled to guiding modes. The guided light emerging at the other end of each waveguide is clearly visible in Fig. 7(c). The green color of the waveguide structure is due to diffracted light from an illumination lamp for the photograph. The guided light in Fig 7(d) was captured by a microscope with a charge-coupled device camera at the plane of the waveguides. Since the guiding modes through the silicon dioxide layer are lossy, light can be guided only along the polymer waveguides.

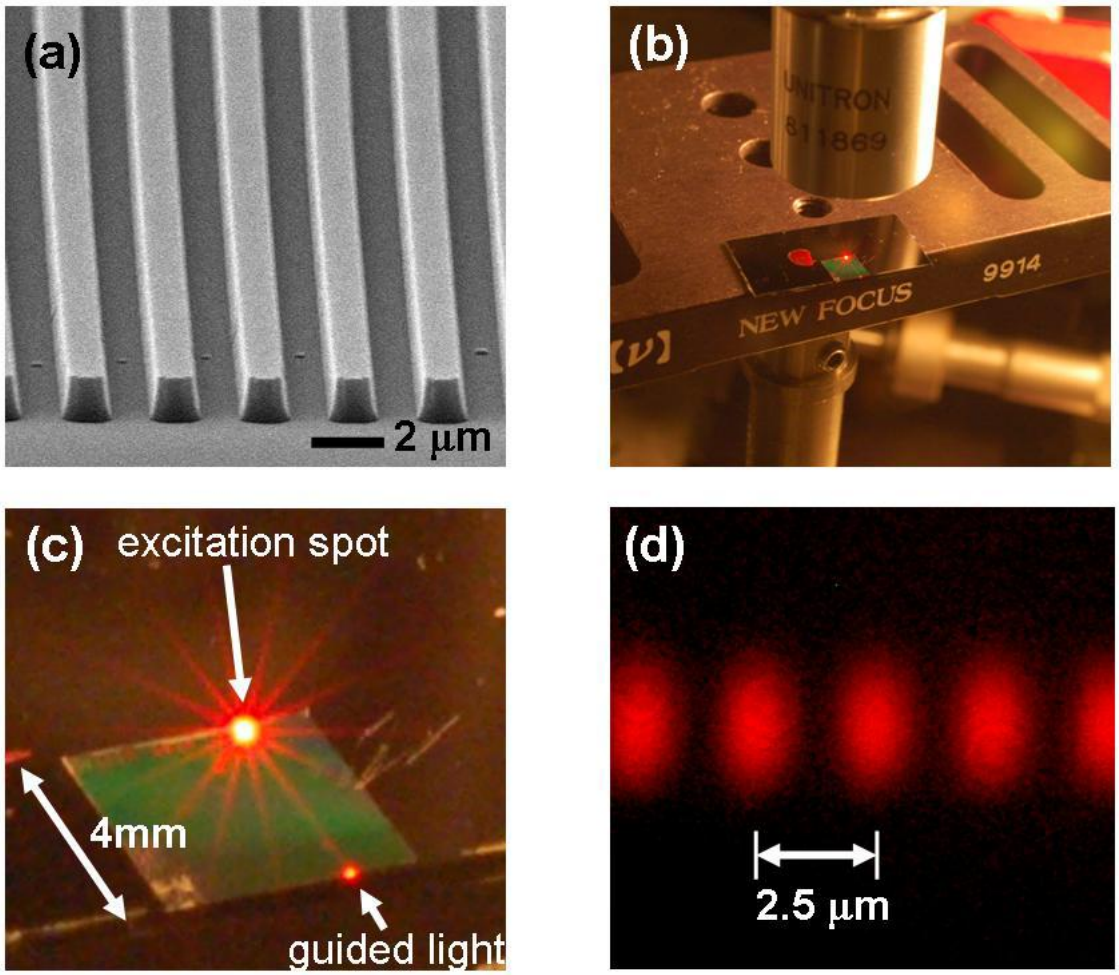

Fig. 7 (a) SEM image of a single layer optical waveguides; (b) Experimental setup for the excitation of the light sources consisting quantum dots; (c) Enlarged optical image of the waveguides structure; (d) Optical microscope image of the guided light.

We also fabricated a waveguide array on a polymeric substrate. The polymeric substrate consists of three layers, the top with a low refractive index, the middle, light absorbing and a base layer. Sufficient refractive index contrast was obtained since the waveguide array and the low refractive index layer have indices of 1.55 and 1.42, respectively. The absorbing layer was added by carbon deposition between the low refractive index and base layer to suppress guiding modes through the polymer substrate. The waveguide array on the polymer substrate was quite flexible in bending because the total thickness of the polymeric substrate was around 50μm. We put the film-like waveguides on a linear stage and each end of the waveguides was attached to a fixed or a movable part of the linear stage. By doing so, we were able to bend the waveguide array as shown in Figure 8(a) and 8(b). A set of quantum dots light sources was embedded with equal spacing at the end of the waveguide array. When the light sources were excited by a UV laser, we were able to observe a series of guided light at the other end of the waveguide array even for the case of bend shown in Fig 8(b). The light guiding characteristics are under investigation with respect to different bending curvatures of the array of waveguides.

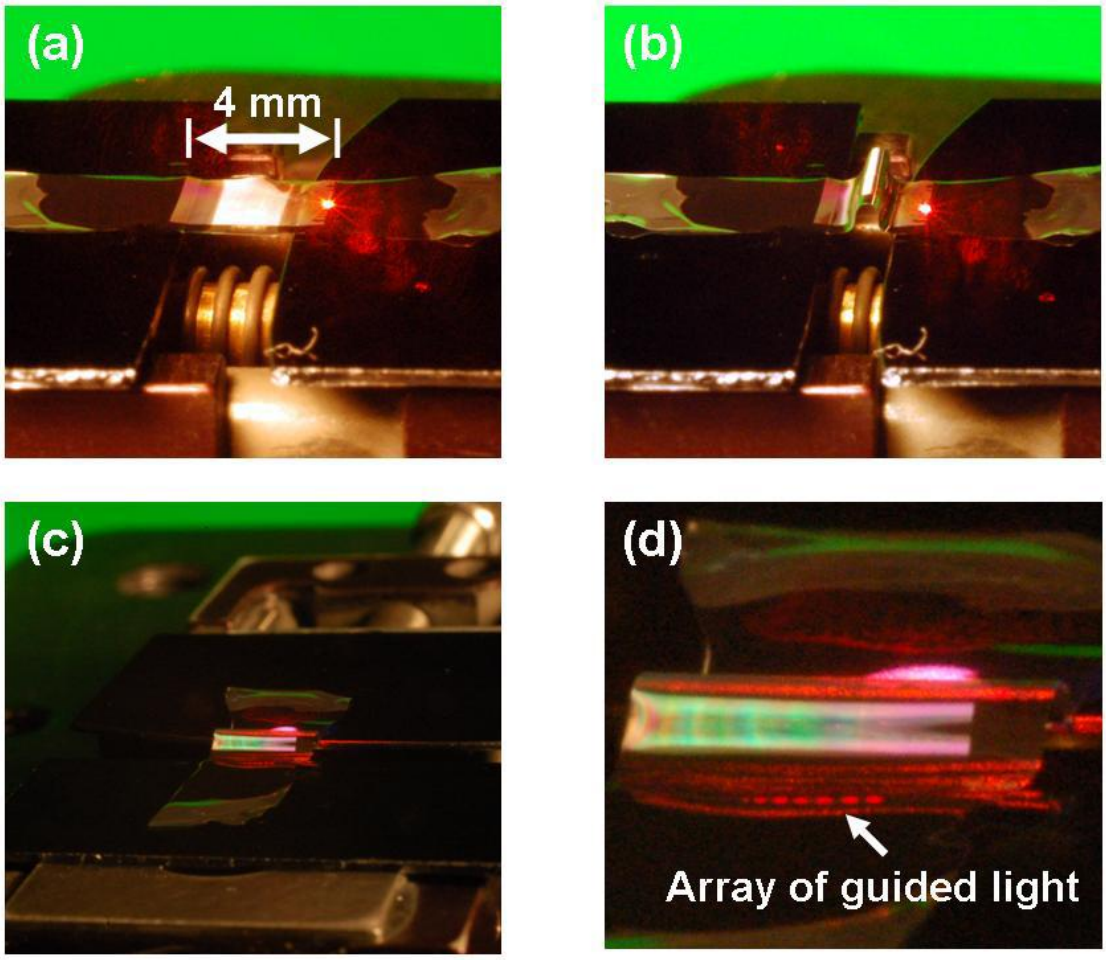

Fig. 8. A flexible array of waveguides is shown (a) before and (b) after bend. (c) Side view along the orientation of waveguides shows that light from the quantum dots propagates along each polymer rod of the array of waveguides when the array is bent. (d) Enlarged view of (c).

3. CONCLUSIONS

We developed an advanced microtransfer molding technique, 2P-μTM to fabricate highly layered polymeric microstructures with both high yield and fidelity. By employing two different UV curable prepolymers, we were able to enhance filling properties while increasing bonding strength between transferred layers. The filling of the structural prepolymer and the selective coating of the bonding prepolymer were achieved by using the WAD process. We also demonstrate that metallic or ceramic photonic crystals could be achievable by conversion of the polymeric templates made by 2P-μTM. The selected structural prepolymer, J-91, can serve as a light-guiding medium by forming micron-scale fibers. The coupling of light sources was readily achieved by depositing quantum-dot resin on an array of waveguides. Although coupling losses of the quantum-dot source and guiding losses of the waveguides have not yet been studied, the fabricated polymeric fiber assembly exhibited waveguide capability in the visible range. By employing sacrificial structures, the waveguide structure can be fabricated in a free-standing form and has potential to achieve three-dimensional optical inter-connections in photonic devices. Moreover, the fabrication technique can be combined with microfluidic systems for lab-on-a-chip applications.

ACKNOLEDGMENTS

This work is supported by the Director for Energy Research, Office of Basic Energy Sciences. The Ames Laboratory is operated for the U. S. Department of Energy by Iowa State University under contract No. W-7405-Eng-82.

REFERENCES

1. S. John, *Phys. Rev. Lett.* **58**, 2486 (1987).
2. S. Y. Lin, J. G. Fleming, D. L. Hetherington, B. K. Smith, R. Biswas, K. M. Ho, M. M. Sigalas, W. Zubrzycki, S. R. Kurtz, and J. Bur, *Nature* (London) **394**, 251 (1998).
3. S. Noda, K. Tomoda, N. Yamamoto, and A. Chutinan, *Science* **289**, 604 (2000).
4. M. Campbell, et al., *Nature* (London) **404**, 53 (2000).
5. Y. A. Vlasov, X. Z. Bo, J. C. Sturm, D. J. Norris, *Nature* (London) **414**, 289 (2001).
6. X. M. Zhao, Y. Xia, G. M. Whitesides, *Adv. Mater.* **1996**, *8*, 837.
7. J. –H. Lee, C. –H. Kim, K. Constant, and K. -M. Ho, Adv. Mater. 17, 2481 (2005).
8. L. Tong, R. R. Gattass, J. B. Ashcom, S. He, J. Lou, M. Shen, I. Maxwell, and E. Mazur, Nature (London) 426, 816 (2003).
9. M. Law, D. J. Sirbuly, J. C. Johnson, J. Goldberger, R. J. Saykally, P. Yang, Science 305, 1269 (2004).
10. D. J. Sirbuly, M. Law, P. Pauzauskie, H. Yan, A. V. Maslov, K. Knusten, C. –Z. Ning, R. J. Saykally, and P. Yang, PNAS 102, 7800 (2005)
11. J. –H, Lee, C. –H. Kim, Y. –S. Kim, K. –M. Ho, K. Constant, W. Leung, C. H. Oh, Appl. Phys. Lett. 2005, 86, 204101.